Exclusion of *Dlx5/6* expression from the distal-most mandibular arches enables BMP-mediated specification of the distal cap

Joshua W. Vincentz[a], Jose J. Casasnovas[a], Ralston M. Barnes[b], Jianwen Que[c], David E. Clouthier[d], Jun Wang[e], and Anthony B. Firulli[a,1]

[a]Riley Heart Research Center, Herman B. Wells Center for Pediatric Research Division of Pediatric Cardiology, Departments of Anatomy, Biochemistry, and Medical and Molecular Genetics, Indiana University Medical School, Indianapolis, IN 46202; [b]Biologics Discovery California, Bristol-Myers Squibb, Redwood City, CA 94063; [c]Department of Medicine, Columbia University Medical Center, New York, NY 10032; [d]Department of Craniofacial Biology, University of Colorado Anschutz Medical Campus, Aurora, CO 80108; and [e]Department of Molecular Physiology and Biophysics, Texas Heart Institute, Baylor College of Medicine, Houston, TX 77030

Cranial neural crest cells (crNCCs) migrate from the neural tube to the pharyngeal arches (PAs) of the developing embryo and, subsequently, differentiate into bone and connective tissue to form the mandible. Within the PAs, crNCCs respond to local signaling cues to partition into the proximo-distally oriented subdomains that convey positional information to these developing tissues. Here, we show that the distal-most of these subdomains, the distal cap, is marked by expression of the transcription factor *Hand1 (H1)* and gives rise to the ectomesenchymal derivatives of the lower incisors. We uncover a *H1* enhancer sufficient to drive reporter gene expression within the crNCCs of the distal cap. We show that bone morphogenic protein (BMP) signaling and the transcription factor HAND2 (H2) synergistically regulate *H1* distal cap expression. Furthermore, the homeodomain proteins distal-less homeobox 5 (DLX5) and DLX6 reciprocally inhibit BMP/H2-mediated *H1* enhancer regulation. These findings provide insights into how multiple signaling pathways direct transcriptional outcomes that pattern the developing jaw.

Bmp | DLX | HAND1 | cranial neural crest cells | development

After migrating to specific locations within the developing embryo, neural crest cells (NCCs), a multipotent cell population originating from the dorsal lip of the neural tube, respond to local morphogenetic signaling cues to pattern and differentiate (1). Following migration to the pharyngeal arches (PAs), cranial NCCs (crNCCs) respond to endothelin 1 (EDN1) and bone morphogenic protein (BMP) signaling from surrounding pharyngeal epithelia to subdivide the PA ectomesenchyme into discrete proximo-distal domains (2). In the mandibular arch (MD1), these nested PA subdomains, characterized by the expression of DLX homeobox and/or HAND basic helix–loop–helix (bHLH) transcription factors, are integral to the development of specific jaw structures, including bone, tongue mesenchyme, and heterogeneous teeth (3). HAND factors regulate mandibular incisor development (4), whereas DLX proteins influence maxillary molar development (2). The mechanisms by which DLX- and HAND-dependent transcriptional programs establish proximo-distal PA subdomains are poorly understood. Indeed, the dearth of identified *cis*-regulatory elements active in postmigratory NCCs has hampered the elucidation of the gene regulatory networks that establish regional identity within the developing mandible.

BMP and EDN1 signaling initially overlaps within the distal murine MD1, but by embryonic day (E)10.5, these signaling pathways become spatially segregated. The distal-most tip of the PAs, known as the distal cap, is transiently devoid of active EDN1 signaling. BMP signaling is ostensibly restricted to this distal cap by the localized expression of Bmp antagonists (3). Here, we provide evidence that DLX5 and DLX6 act as transcriptional repressors of BMP signaling specifically within the cranial PAs. We show that, within the crNCCs, the BMP-dependent transcription factors

Smads, H2, and GATA2/3 provide positive transcriptional inputs that serve to counteract the activity of Dlx proteins, thereby relieving EDN1-mediated repression. Together, these findings integrate the communication between BMP and EDN1 signaling that establishes the distal cap of the mandible.

Results

The H1^Cre Lineage Gives Rise to the Lower Incisors, in a HAND Factor-Dependent Manner. *H1* expression is confined to the distal cap ectomesenchyme (4, 5). *H1* dimer mutants display noncell-autonomous craniofacial phenotypes outside of the distal cap (6). The *H1^Cre* knock-in allele provides a tool with which to interrogate cell-autonomous roles of Hand factors in the MD1 (7, 8). To examine the development of the *H1* lineage relative to the developing incisors, we performed X-Gal staining of *R26R^lacZ/+;H1^Cre/+* embryos at E15.5. Consistent with *H1^lacZ* expression, the *H1* lineage is restricted to the midline of the tongue and Meckel's cartilage within the developing jaw; however, the dental papilla (dp) of the mandibular incisors, which exhibits undetectable *H1^lacZ* expression (4) (Fig. S1*A*) is derived from *H1^Cre*-marked cells (Fig. S1*B*). These findings suggest that Hand factors function cell-autonomously during early mandibular incisor development.

Significance

Within the developing mandible, proper specification and positioning of bone, tongue, and teeth are controlled by secreted morphogens. Among these morphogenetic cues, endothelin 1 (EDN1) and bone morphogenic proteins (BMPs) divide the nascent mandible into subdomains along a proximo-distal axis. The transcriptional mechanisms by which mandibular progenitor cells interpret morphogenetic signals to establish these subdomains are poorly understood. Here, we characterize a *Hand1* enhancer that drives gene expression specifically within the distal-most of these subdomains, the distal cap. Our findings show that Bmp-dependent transcription factors provide positive transcriptional inputs that serve to counteract the repressive activity of EDN1-dependent transcription factors within the distal cap, thus integrating the communication between BMP and EDN1 signaling that patterns the mandible.

To test this hypothesis, we generated $H1^{Cre}$;$H2$ conditional knockouts (CKOs) within the distal cap (Fig. S1 C–E). Because the $H1^{Cre}$ allele is a knock-in, the resulting embryos are both null for $H2$ and heterozygous for $H1$ within these cells. Histological and marker analyses show that, in contrast to E12.5 control embryos, in which thickened dental laminae of two prospective incisors are evident in the mandible (Fig. S1 F, H, and J, arrowheads), a single, arrested lamina is observed in $H2^{fx/-}$;$H1^{Cre/+}$ CKOs (Fig. S1 G, I, and K, arrowheads). Collectively, these data show that distal cap $H1$-lineage cells within the MD1 compose a subdomain of the ectomesenchymal component of the mandibular incisors in a HAND factor-dependent manner.

A H1 Distal Cap Enhancer Is Located Within a 443-Bp Bmp-Responsive Element.

To characterize the transcriptional mechanisms that define distal cap, we used promoter deletion analyses to identify the cis-regulatory elements that drive $H1$ gene expression within crNCCs. Comparative genomic analyses identified conserved noncoding regions (>75% conserved between mouse and human across >100 bp; red boxes in Fig. 1A; ref. 9); that were isolated and assayed for enhancer activity via transgenic reporter analysis. F_0 transgenic analyses identified a 2.4-kb enhancer sufficient to drive gene expression in both crNCCs and cardiac NCCs (caNCCs; $n = 16/20$), as well as the myocardial cuff (MC; $n = 16/20$), and septum transversum (ST; $n = 15/20$) consistent with expression of $H1^{lacZ}$ and $H1^{Cre}$ alleles (Fig. 1 G–K) (7, 8, 10).

BMP4 lies upstream of $H1$ in NCCs (11, 12). $Bmp7$ knockouts display mandibular incisor phenotypes similar to $Hand$ factor mutants (13). To test the BMP responsiveness of this full-length $H1$ enhancer, it was cloned into a luciferase (luc) reporter construct (#13; Fig. 1L). Construct #13 was cotransfected with constitutively active BMP type I receptors (caBmpr1a or caBmpr1b) and BMP transcriptional effectors (Smad1 or Smad5, and Smad4). BMP robustly up-regulated Construct #13 (Fig. 1M). Deletion analyses reveal that the 3′ 1.0 kb of the $H1$ enhancer is BMP-responsive, whereas the remaining 5′ 1.4 kb of $H1$ enhancer sequence is not (Fig. 1M; #15 and #14). Serial deletions of Construct #15 (Fig. 1L) revealed a 443-bp fragment (Construct #20; Fig. 1L, green highlight) sufficient to convey BMP responsiveness (Fig. 1N).

We next tested whether this 443-bp Bmp-responsive element is sufficient to drive gene expression in NCCs (Fig. 1O). X-Gal staining of four independent E10.5 F_0 embryos confirmed that the 443-bp Bmp-responsive element (Fig. 1O, green) was sufficient to drive robust reporter expression within the crNCCs (Fig. 1Q, white arrowhead), caNCCs (Fig. 1R, white arrow), and MC (Fig. 1R, black arrow) in a domain comparable to that of endogenous $H1$ (Fig. 1 B–F). X-Gal staining was not observed within the ST or lateral mesoderm (LM). The remaining 5′ most fragment (Construct #21) drove only ST-specific gene expression (Fig. 1 T–W, black arrowhead). Thus, the 443-bp $H1$ enhancer ($H1^{PA/OFT}$ enhancer) is BMP-responsive and sufficient to drive gene expression within postmigration NCCs and the MC.

Smad Factors Directly Regulate the H1^PA/OFT Enhancer to Define the Distal Cap.

To test whether BMP signaling directly regulates the $H1^{PA/OFT}$ enhancer, we individually mutagenized four putative SMAD cis elements (14, 15) (numbered 1–4, Fig. S2) in luc-reporter constructs corresponding to Construct #15 (Fig. 2A). Mutation of the 5′-most Smad site (15.S1) reduced BMP responsiveness by 44%. Individual mutation of each of the remaining three Smad binding sites (15.S2, S3, and S4) eliminated BMP responsiveness (Fig. 2B). P-SMAD1/5/8 chromatin immunoprecipitation (ChIP) from isolated E10.5 facial primordia confirmed that P-SMAD1/5/8 binds within this $H1$ genomic region (Fig. 2C). We next mutagenized the 3′ critical sites within the full-length 2.4-kb reporter construct (Construct #13.S2-4; Fig. 2D), showing that resulting F0 embryos lack lacZ expression in NCCs (Fig. 2 E–H). Abolishing BMP responsiveness within NCCs by conditionally deleting Smad4 (Smad4 NCC CKO) revealed that Construct #20 reporter transgene expression requires SMAD4 (Fig. 2 M–P). Conversely, NCC-specific expression of a constitutively active Bmpr1a (ref. 16; Bmpr1a NCC ca) caused proximally expanded NCC Construct #20 expression (Fig. 2 Q–T). These findings establish that the $H1^{PA/OFT}$ enhancer is directly regulated through SMAD-mediated BMP signaling.

H2 Acts Synergistically with Smads to Directly Regulate the H1^PA/OFT Enhancer.

BMPs directly regulate $Msx2$ expression within the PAs (17). $Msx2$ expression is broader than $H1$, hinting that additional transcription factors regulate each gene. $H1$ expression is lost in crNCCs when $H2$ is ablated (18). Luc assays using Construct #15 indicated that, although H2 is not sufficient to up-regulate $H1^{PA/OFT}$ enhancer expression on its own, H2 synergizes with BMP signaling to up-regulate expression ~threefold greater than BMP alone (Fig. 3A). We next sought to genetically and molecularly characterize H2 and SMAD interactions. Although H2 loss-of-function does not disrupt BMP signaling in the PAs, H2
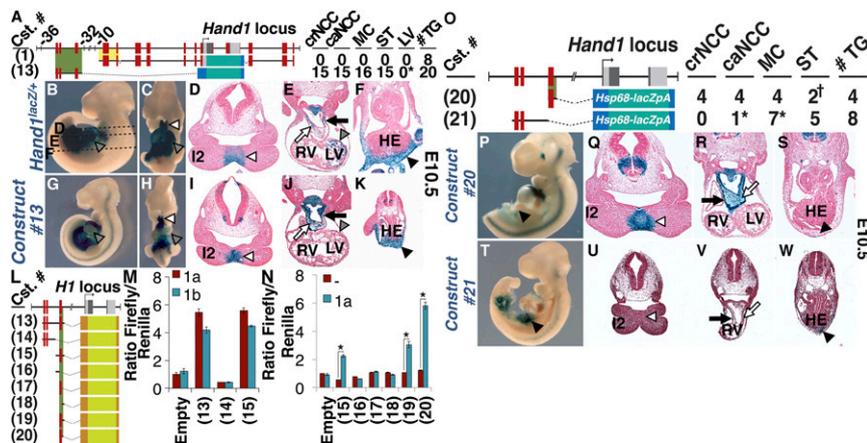

Fig. 1. A 443-bp BMP-responsive $H1$ cis-regulatory element drives gene expression in NCC and MC. (A) Murine $H1$ locus and reporter constructs. Red boxes indicate regions of genomic conservation. (B–K) X-Gal staining of an E10.5 $H1^{lacZ/+}$ embryo (B–F) and Construct #13 F_0 transgenic reporter (G–K) in whole mount (B, C, G, and H) and transverse section (D–F, I, and J). (L) Schematic of Construct #13–Construct #20. (M and N) Luc assays show the 443-bp Construct #20 conveys BMP responsiveness. 1a, caBmpr1a; 1b, caBmpr1b. (O) Transgene reporter Constructs #20 and #21. (P–W) X-Gal staining of F_0 Construct #20 (P–S) and #21 (T–W) transgenics in whole-mount (P and T) and transverse sections (Q–S and U–W). Dashed lines in B denote level of sections in D–F. *, punctate expression; †, broad expression in the ST; HE, hepatic endoderm; I2, MD1; LV, left ventricle; RV, right ventricle; #TG, number of F_0s.
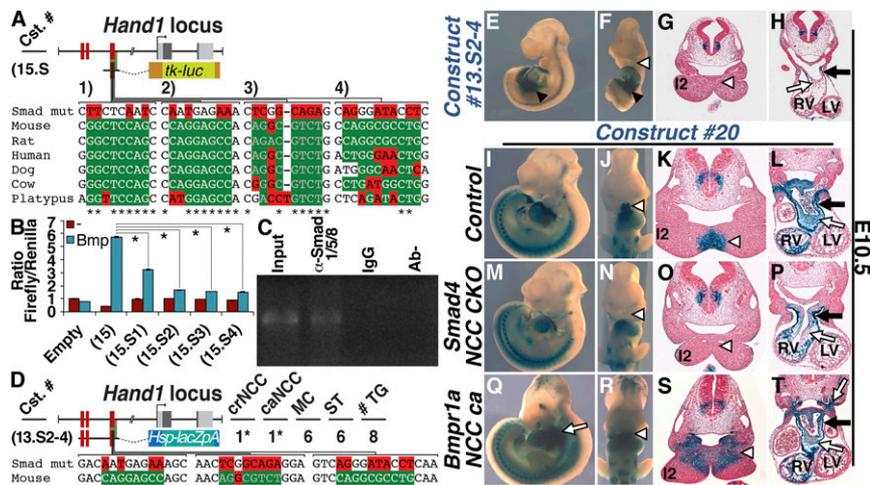
Vincentz et al.

www.manaraa.com

Fig. 2. Mutation of $H1^{PA/OFT}$ Smad *cis* elements abolishes responsiveness to BMP. (*A*) Each of four conserved SMAD consensus motifs (green) have been individually mutagenized in *Construct #15* (*Constructs #15.S1-4*). (*B*) *Luc* assays show that SMAD site mutation either reduces (15.S1) or abolishes (15.S2, S3, and S4) BMP-responsiveness. (*C*) ChIP from E10.5 facial primordia confirms SMAD DNA occupancy. (*D*) *H1* locus and *Construct #13.S2-4* in which the SMAD sites 2–4 are mutagenized within *Construct #13*. (*E–T*) X-Gal staining of F₀ *Construct #13.S2-4* (*E–H*) *Construct #20* line bred onto a *Control* (*I–L*), a NCC-specific *Smad4 NCC CKO* (*M–P*), or *Bmpr1a NCC ca* (*Q–T*). *, weak expression. I2, MD1; LV, left ventricle; RV, right ventricle.

and BMP signaling does converge to regulate the expression of a subset of distal cap target genes (11) (Fig. S3 *C–L*). Coimmunoprecipitation experiments revealed that H2 interacts with SMAD1 (Fig. S3*M*). To confirm that H2 directly binds to the $H1^{PA/OFT}$ enhancer, we identified E-box and D-box consensus motifs (19) (Fig. S2, turquoise and dark red). Three pairs of palindromic D boxes overlapped with SMAD *cis* elements 2–4 (Fig. S2, dark blue). Electrophoretic mobility shift assays (EMSAs) confirmed specific H2-E12 heterodimer binding to each of these D boxes (Fig. S3 *P–R*). Published H2 ChIP-Seq data confirms significant enrichment within the $H1^{PA/OFT}$ enhancer (20). These data support that H2 and SMAD1 are components of a transcriptional complex that directly regulates the $H1^{PA/OFT}$ enhancer.

The proximity of the D boxes and SMAD *cis* elements 2–4 precluded mutagenizing these sites to confirm their necessity; however, crNCC expression of *Construct #20* was lost when bred onto a *H2CKO* background (Fig. 3 *E* and *F*, white arrowhead), whereas MC (Fig. 3*G*, black arrow) and, importantly, caNCC (Fig. 3*G*, white arrow) expression was unaffected.

We next hypothesized that H2 functions in the MD1 to inhibit a Bmp antagonist. *Twist1* is broadly expressed in crNCCs within the MD1, but is excluded from the distal cap (21, 22). TWIST1 inhibits BMP signaling within the forming cranial sutures (23) and antagonizes H2 within the developing limb (24). Although *Construct #20* crNCC reporter expression did appear broader in the PAs of E10.5 *Twist1^fx/+;Wnt1-Cre(+)* embryos (Fig. S4), the PAs are markedly dysmorphic (25), complicating interpretation. In contrast, conditional *Twist1* overexpression within NCCs using a *CAG-CAT-Twist1* allele (26, 27) caused a loss of *Construct #20* crNCC reporter expression (Fig. 3 *H* and *I*, white arrowhead). Importantly, caNCC $H1^{PA/OFT}$ enhancer expression was unaffected by altered *Twist1* expression (Fig. 3 *G* and *J* and Fig. S4). *Twist1* is endogenously expressed in caNCCs within the OFT (21). Thus, if TWIST1 functioned as the primary BMP antagonist, H2 inactivation would result in the loss of $H1^{PA/OFT}$ enhancer activity in both crNCCs and caNCCs.

Dlx5/6 Antagonizes Bmp Responsiveness of the $H1^{PA/OFT}$ Enhancer. DLX5/6 are induced by EDN1 signaling and directly regulate *H2* expression within the rostral PAs (28). H2 then feeds back to repress both *Dlx5/6* expression within the distal cap (18). Although *Dlx5/6* are both expressed in crNCCs, neither is expressed in caNCCs (29, 30). We therefore explored the regulatory influence of

DLX5/6 on the $H1^{PA/OFT}$ enhancer. *Luc* assays showed that both Dlx5/6 strongly antagonized H2/BMP $H1^{PA/OFT}$ enhancer *trans* activation (Fig. 4*A*).

If DLX5/6 represses the $H1^{PA/OFT}$ enhancer in vivo, it would follow that BMPs and/or H2 must antagonize these factors within the distal cap. In situ hybridization showed that *H2* expression is lost in NCC-specific *Smad4* CKOs (Fig. 4*C*). Conversely, *Dlx5* expression, which is normally excluded from distal cap crNCCs, expanded, and was uniformly expressed throughout the PAs in these CKOs (Fig. 4*E*). We have reported that a similar distal expansion of *Dlx5/6* occurs in *H2CKO* mice along with loss of *H1* expression (18). We reasoned that H1 could be necessary for restriction of *Dlx5/6*; however, examination of *Dlx5/6* in NCC *H1CKOs* revealed no changes in expression domain (Fig. S5). We next investigated whether activating BMP signaling antagonizes *Dlx5* expression. As expected, *H1* expression expanded proximally in the NCCs of *Bmpr1a ca* embryos (Fig. 4*G*). Consistent with a model in which DLX5/6 restricts *H1* expression to the distal cap, *Dlx5* (Fig. 4*I*) expression was further restricted within the proximal PAs in *Bmpr1a NCC ca* embryos.

We next asked whether DLX proteins directly mediate BMP antagonism. No homeodomain consensus sequences (31) were found within the $H1^{PA/OFT}$ enhancer, so we divided the enhancer into five 89-bp fragments and assessed DLX5 binding by EMSA. DLX5 directly binds to three discrete sites within this sequence (Fig. 4*J*). DLX3 binds the consensus site (ACG)TAATT(GA)(CG) (32). Two similar sites, referred to as DLX 5′ and DLX 3′, appear within the $H1^{PA/OFT}$ enhancer (Fig. S2). EMSAs confirmed direct DLX5 DNA binding (Fig. 4*J*). The third DLX5 binding site overlaps with a GATA consensus site (*Dlx/Gata 5′*), located directly 5′ to the Smad site 3 (Fig. S2 and Fig. 4*J*). Mutation of these sites ablated their ability to compete for DLX5 DNA binding (Fig. 4*J*) and ablated DLX5 direct DNA binding (Fig. S6*A*).

We next interrogated whether these DLX-binding sites are required to confer transcriptional repression. Mutation of the 5′-most site, *Dlx 5′*, had no effect upon DLX-mediated repression (Fig. S6*B*). Mutation of the 3′-most site, *Dlx 3′*, also did not affect DLX-mediated repression, but instead diminished Bmp responsiveness (Fig. S6*B*). Mutation of *Dlx/Gata 5′* eliminated BMP responsiveness (Fig. S6*B*). Thus, we cannot conclude that these DLX-binding sites are required for transcriptional repression, because positive transcriptional regulators require these sites to *trans*-activate $H1^{PA/OFT}$.
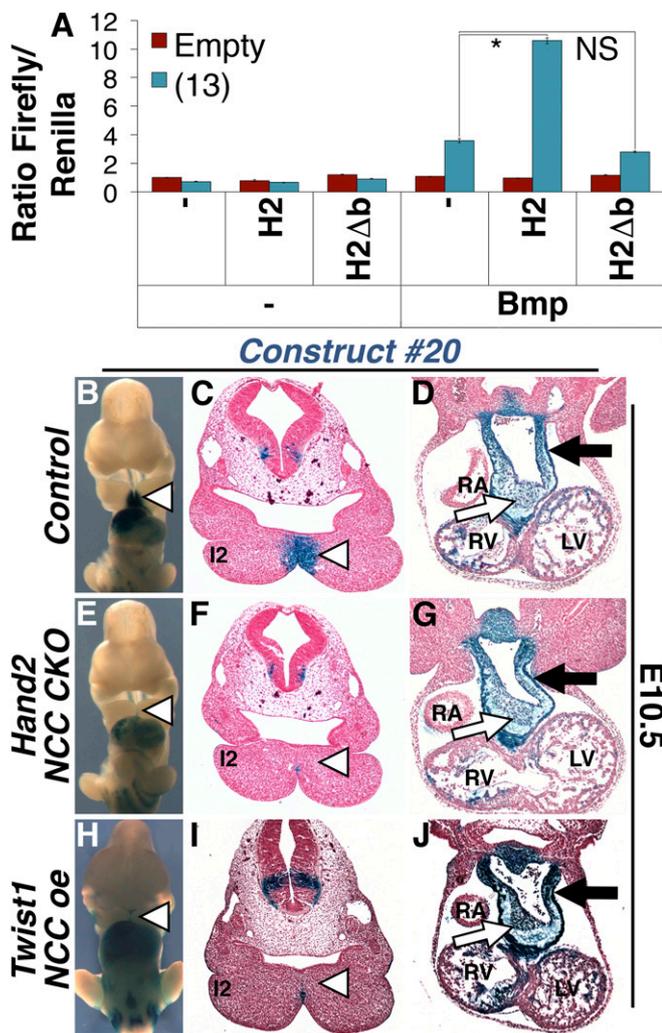
Vincentz et al.

DEVELOPMENTAL BIOLOGY

Fig. 3. H2 and Twist1 directly modulate Bmp-mediated $H1^{PA/OFT}$ expression. (*A*) *Luc* assays show that H2 by itself has no transcriptional effect on the *H1* enhancer; however, H2 and activated BMP signaling synergistically up-regulate *luc* reporter expression ~threefold over BMP transactivation alone. A DNA binding-deficient H2 mutant (H2Δb) does not synergize. (*B–J*) X-Gal staining of the *Construct #20* transgenic reporter line bred onto a *Control* (*B–D*), NCC-specific *H2CKO* (*E–G*), or onto a NCC-specific *Twist1*-over-expressing background (*H–J*). I2, MD1; LV, left ventricle; RA, right atrium; RV, right ventricle.

Gata Factors Are Necessary for H1$^{PA/OFT}$ Enhancer Activity Within the Distal Cap. We sought to identify the transcriptional regulator(s) that up-regulate the $H1^{PA/OFT}$ enhancer via elements overlapping with the DLX *cis* elements. The DLX binding site *Dlx/Gata* 5′ is required for *trans* activation. This site and a second, 3′ GATA *cis* element flank SMAD site 3 (Fig. S2). GATA2 and GATA3 are related transcription factors important for jaw development (22, 33) and for proper *H2* and *Dlx5* PA expression (22). Importantly, *Gata2/3* PA expression is BMP-dependent (11).

We tested whether these GATA *cis* elements are required for $H1^{PA/OFT}$ enhancer activity. We performed *luc* assays, observing that individual mutation of either of these sites abolished BMP responsiveness in vitro (Fig. 4*K*). EMSA confirmed that GATA2/3 bound to both $H1^{PA/OFT}$ enhancer GATA sites (Fig. 5*A*). We next generated transient transgenics in which the GATA sites have been mutated. These F$_0$ embryos displayed a complete loss of $H1^{PA/OFT}$ enhancer activity within crNCCs but displayed expression within caNCCs (Fig. 5*C*). These results support a model wherein positive

GATA factor inputs directly drive $H1^{PA/OFT}$ enhancer activity, precluding assessment of their requirement for *H1* repression.

Discussion

We identify a complex *H1* enhancer, which models the transcriptional mechanisms that define the distal cap of the rostral PAs (Fig. S7). The distal cap domain, in turn, gives rise to the mandibular incisor ectomesenchyme. These studies are the first to our knowledge to demonstrate that cells within the distal cap of MD1 directly contribute to the mandibular incisors. These findings expand on published reports (4), and reveal that loss of HAND factors does not disrupt mandibular incisor development via defective midline development, but rather disrupts the development of a key cell-lineage necessary for lower incisor morphogenesis. Given that *H1* crNCC transcriptional regulation directly depends on BMP signaling, and this *H1* lineage coincides with the distal cap domain, we conclude that *H1* marks the distal cap and its lineage is required for mandibular incisor formation. Indeed, *Bmp7* mutants show similar incisor defects (13), and both *H1* and *H2* are down-regulated in *Bmp4CKOs* (11). Increased BMP signaling results in both an up-regulation of *H1* and *H2* and MD1 incisor abnormalities (11, 34). Moreover, *H2* NCC CKOs exhibit fused, hypoplastic incisors (18), whereas *H1* is not required for incisor development, because NCC *H1CKOs* displays no phenotypes (4), and does not affect the *Dlx5/6* distal cap expression (Fig. S5). *H1* haploinsufficiency on a *H2CKO* background yields a single lower incisor (Fig. S1), revealing a HAND factor dosage relationship. Indeed, loss of *H2* within the MD1 does not alter SMAD1/5/8 phosphorylation, but alters *H1* expression and allows for *Dlx5/6* expansion into the distal cap (Fig. 3 and Fig. S3) (18). Because *Hand* expression is lost in *Smad4CKOs*, it is unclear whether SMAD factors themselves directly contribute to *Dlx5/6* repression. SMADS are clearly not sufficient for *Dlx5/6* repression; rather, it is the cooperative overlap of BMP signaling and HAND factor expression that defines the distal cap. This observation reframes mandibular patterning in the context of the BMP/H2-defined distal cap cell lineage, rather than gene expression within the PA primordia.

The mechanisms uncovered in this study show that positive and negative feedback regulation, initiated through the EDN1-induced endothelin receptor A (EDNRA) signaling cascade, ultimately pattern the distal cap of MD1. Within crNCCs, EDNRA function is required for the expression of *Dlx5/6* and *Bmp4* (22). DLX5/6 are then required for *H2* expression (28). Although DLX5/6 exert a repressive influence upon the $H1^{PA/OFT}$ enhancer, DLX5/6 are required to up-regulate H2, a necessary *H1* trans activator (Fig. 3; ref. 18). This indicates that the reduced *H1* expression observed in the distal cap of $Dlx5/6^{-/-}$ mutants (35) results from the loss of H2 (Fig. 3 *E–G*). Furthermore, EDNRA is necessary to exclude *Twist1* expression from the distal cap (22). These findings support a TWIST1/H2-mediated negative-feedback loop that proximally expands the BMP signaling domain and restricts the EDN1 signaling domain.

EDNRA signaling components are thought to be transcriptionally downstream of GATA2/3 (36). In support of this, *Gata3* expression is unperturbed by the disruption of EDNRA signaling (22). However, BMP4 regulates *Gata3* expression in the MD1 (11). The findings reported here demonstrate that these factors exert either positive (BMP, H2, Gata2/3) or negative (TWIST1, DLX5/6) influences upon *H1* transcription, thereby restricting *H1* expression to the distal cap (Fig. S7).

The Hinge and Caps model of proximo-distal domain specification within the MD1 posits a combination of transcriptional cross-talk and positive and negative feedback among EDNRA, BMP, and FGF signaling (1, 3, 37). In this model, EDN1 and Bmps have overlapping distal cap functions, but as PA development proceeds, their functions resolve into distinct intermediate and distal domains. The BMP antagonists GREMLIN2, CHORDIN,
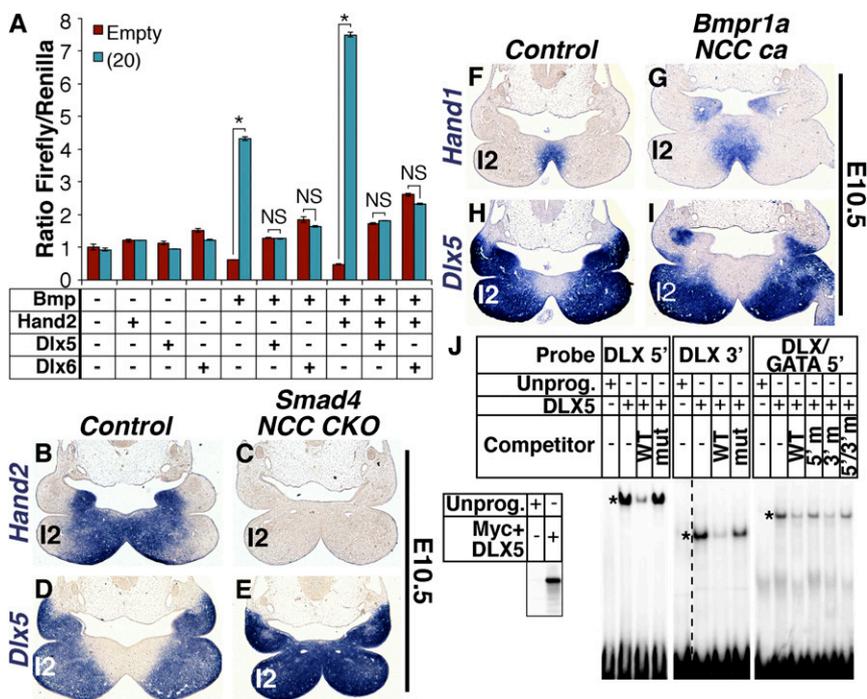
Fig. 4. Dlx5/6 represses the $H1^{PA/OFT}$ enhancer within crNCCs. (A) Luc assays show that DLX5/6 represses H2/BMP synergistic activation of the $H1^{PA/OFT}$ enhancer. (B–E) In situ hybridization shows that crNCC H2 expression (B and C) is lost in Smad4CKOs, whereas Dlx5 expression (D and E) is uniformly expressed throughout MD1. (F–I) H1 expression is expanded proximally in caBmpr1a F_0 embryos (F and G) and Dlx5 expression (H and I) is further restricted to the proximal PAs. (J) EMSAs show that DLX5 can bind to three discrete sites within the H1 enhancer. *, bound DNA complexes. Dotted lines denote where gel lanes were rearranged. Unlabeled competitors are as follows: 5'm, DLX/GATA 5'mut; 3'm, GATA 3'mut; 5'/3' m, DLX/GATA 5', GATA 3'mut; I2, MD1mut; mutant; WT, wild-type.

and NOGGIN are proposed to regulate this transcriptional resolution (3). The PA domain of BMP signaling responsiveness is presumed to be regulated at the chromatin level such that high levels of Bmp signaling are required for SMAD factors DNA binding (11). Indeed, in fish, high levels of exogenous Bmps can rescue h2 expression in $edn1^{-/-}$ mutants (3). Here, we report that the EDNRA signaling effectors DLX5/6 can transcriptionally antagonize BMP signaling. These findings provide new insight into the mechanism by which Bmp and EDNRA signaling, initially redundant in the distal PAs, use cross-inhibitory interactions to become spatially and functionally segregated during PA development.

At the hinge, FGF8 signaling establishes both anterior-posterior and proximo-distal polarity (1, 37). Importantly, FGF8 is partially required for expression of both Edn1, which is solely a proximo-distal morphogen, and Dlx1, which establishes the most proximal domain of MD1. These studies reveal that early specification of MD1 progenitors by hinge signals and/or by the

homeostatic integration of hinge and cap signaling segregates EDN1/EDNRA- and BMP-signaling programs, orchestrating proximo-distal MD1 patterning. BMP4 both activates and represses Fgf8 expression dosage-dependently (38). It is likely that the disruption of BMP signaling and downstream BMP targets such as H1 and H2 feeds back upon Fgf8 hinge expression. Indeed, in H1 dimer mutants, Fgf8 levels are markedly increased (6).

Finally, this study is the first to our knowledge to draw defined distinctions between the transcriptional pathways active in crNCCs and caNCCs postmigration. These studies show that BMP signaling is required for $H1^{PA/OFT}$ enhancer up-regulation in both cell populations; however, Dlx5/6 antagonism only occurs in crNCCs, not caNCCs. As such, H2 inputs are required to antagonize DLX repression in crNCCs (18), but are dispensable for $H1^{PA/OFT}$ enhancer activity in caNCCs. This transcriptional divergence is key to our understanding of how, despite similarities, crNCC fate determination ultimately drives these cells to form, primarily, bone and connective tissue, whereas, caNCCs ultimately form, primarily, smooth muscle.
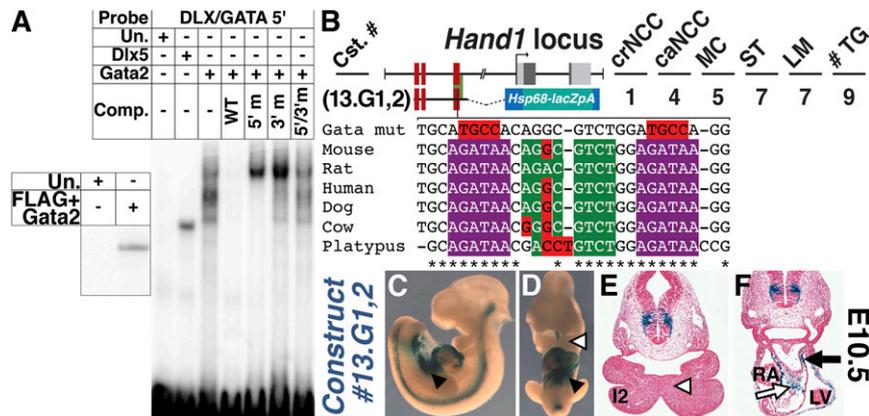

Fig. 5. Mutation of Gata cis-binding elements in the $H1^{PA/OFT}$ enhancer disrupts expression in crNCCs. (A) EMSAs show that GATA2 binds to both H1 enhancer GATA sites. (B) H1 locus and Construct #13.G1,2-containing GATA mutants within the context of Construct #13. (C–F) X-Gal staining of F_0 Construct #13.G1,2. I2, MD1; LV, left ventricle; RV, right ventricle.

Vincentz et al.

Materials and Methods

Transgenic Mice. Genotyping of all alleles was performed as described and is detailed in *SI Materials and Methods* and Tables S1 and S2.

Cloning. The 2.4-kb *H1* enhancer, corresponding to −34,680 to −32,285 bp from the transcription start site, was amplified from genomic DNA by using the primers BoxZ(F/XhoI); 5′-AATCTCGAGCAATCCTGATTCCTCTGC-3′ and BoxZ(R/SalI); 5′-GCAGTCGACTTCATCACAAAGGGGAAG-3′, and subcloned into pCRII-TOPO (Thermo Fisher). *Luc* and *β-galactosidase* reporter constructs are detailed in *SI Materials and Methods* and Table S3.

X-Gal Staining. X-Gal staining of whole-mount and sectioned embryos was performed as described (7, 10). All embryo sections are transverse unless otherwise indicated.

In Situ Hybridization. Section in situ hybridizations were performed on 10-μm paraffin sections as described (21). Digoxygenin-labeled riboprobes were synthesized by using T7, T3, or SP6 polymerases (Promega) and DIG-Labeling Mix (Roche). Probe templates are detailed in *SI Materials and Methods*.

Immunohistochemistry. Immunohistochemistry was performed as described (21) α-P-SMAD1/5/8 (AbCam) and DyLight secondary (Thermo Scientific) antibodies were used.

Immunoblotting and Coimmunoprecipitation Experiments. Coimmunoprecipitation experiments were performed in CaPO$_4$-transfected HEK 293 cells by using α-Myc and α-Flag (Sigma) as described (39).

Transactivation Assays. Luciferase assays were performed in CaPO$_4$-transfected HEK293 cells as described (19). Error bars denote SE. Asterisks denote $P \leq 1.0 \times 10^{-3}$. NS, not significant.

Bioinformatics. Sequences were obtained by Ensembl BLASTN search (www.ensembl.org) against human *H1* sequence. PATTERNMATCH and CLUSTALW analyses used the San Diego Supercomputer Center Biology Workbench (workbench.sdsc.edu).

EMSA. EMSAs were performed as described (27) by using the TnT rabbit reticulocyte lysate in vitro transcription system (Promega). $\gamma^{32}P$ ATP 5′ end-labeled double-stranded probes were mixed with 1 μg of poly(dG-dC) and either specific or nonspecific unlabeled DNA-binding oligos. Reactions were incubated for 30 min at room temperature and run on nondenaturing gels. Gels were dried and phosphoimaged.

Ethics Statement. Mouse experiments follow approved animal protocol 10809 from the Indiana University Institutional Animal Care and Use Committee.

1. Schilling TF, Le Pabic P (2014) *Neural Crest Cells in Craniofacial Skeletal Development A2 - Trainor, Paul A. Neural Crest Cells* (Academic, Boston), pp 127–151.
2. Chai Y, Maxson RE, Jr (2006) Recent advances in craniofacial morphogenesis. *Dev Dyn* 235(9):2353–2375.
3. Medeiros DM, Crump JG (2012) New perspectives on pharyngeal dorsoventral patterning in development and evolution of the vertebrate jaw. *Dev Biol* 371(2):121–135.
4. Barbosa AC, et al. (2007) Hand transcription factors cooperatively regulate development of the distal midline mesenchyme. *Dev Biol* 310(1):154–168.
5. Yanagisawa H, Clouthier DE, Richardson JA, Charité J, Olson EN (2003) Targeted deletion of a branchial arch-specific enhancer reveals a role of dHAND in craniofacial development. *Development* 130(6):1069–1078.
6. Firulli BA, Fuchs RK, Vincentz JW, Clouthier DE, Firulli AB (2014) Hand1 phosphor-egulation within the distal arch neural crest is essential for craniofacial morphogenesis. *Development* 141(15):3050–3061.
7. Barnes RM, Firulli BA, Conway SJ, Vincentz JW, Firulli AB (2010) Analysis of the Hand1 cell lineage reveals novel contributions to cardiovascular, neural crest, extra-embryonic, and lateral mesoderm derivatives. *Dev Dyn* 239(11):3086–3097.
8. Barnes RM, et al. (2011) Hand2 loss-of-function in Hand1-expressing cells reveals distinct roles in epicardial and coronary vessel development. *Circ Res* 108(8):940–949.
9. Vincentz JW, et al. (2012) A Phox2- and Hand2-dependent Hand1 cis-regulatory element reveals a unique gene dosage requirement for Hand2 during sympathetic neurogenesis. *J Neurosci* 32(6):2110–2120.
10. Firulli AB, McFadden DG, Lin Q, Srivastava D, Olson EN (1998) Heart and extra-embryonic mesodermal defects in mouse embryos lacking the bHLH transcription factor Hand1. *Nat Genet* 18(3):266–270.
11. Bonilla-Claudio M, et al. (2012) Bmp signaling regulates a dose-dependent transcriptional program to control facial skeletal development. *Development* 139(4):709–719.
12. Howard MJ, Stanke M, Schneider C, Wu X, Rohrer H (2000) The transcription factor dHAND is a downstream effector of BMPs in sympathetic neuron specification. *Development* 127(18):4073–4081.
13. Zouvelou V, Luder HU, Mitsiadis TA, Graf D (2009) Deletion of BMP7 affects the development of bones, teeth, and other ectodermal appendages of the orofacial complex. *J Exp Zoolog B Mol Dev Evol* 312B(4):361–374.
14. Zawel L, et al. (1998) Human Smad3 and Smad4 are sequence-specific transcription activators. *Mol Cell* 1(4):611–617.
15. Morikawa M, et al. (2011) ChIP-seq reveals cell type-specific binding patterns of BMP-specific Smads and a novel binding motif. *Nucleic Acids Res* 39(20):8712–8727.
16. Rodriguez P, et al. (2010) BMP signaling in the development of the mouse esophagus and forestomach. *Development* 137(24):4171–4176.
17. Brugger SM, et al. (2004) A phylogenetically conserved cis-regulatory module in the Msx2 promoter is sufficient for BMP-dependent transcription in murine and Drosophila embryos. *Development* 131(20):5153–5165.
18. Barron F, et al. (2011) Downregulation of Dlx5 and Dlx6 expression by Hand2 is essential for initiation of tongue morphogenesis. *Development* 138(11):2249–2259.
19. Firulli BA, Redick BA, Conway SJ, Firulli AB (2007) Mutations within helix I of Twist1 result in distinct limb defects and variation of DNA binding affinities. *J Biol Chem* 282(37):27536–27546.
20. Osterwalder M, et al. (2014) HAND2 targets define a network of transcriptional regulators that compartmentalize the early limb bud mesenchyme. *Dev Cell* 31(3):345–357.
21. Vincentz JW, et al. (2008) An absence of Twist1 results in aberrant cardiac neural crest morphogenesis. *Dev Biol* 320(1):131–139.
22. Ruest LB, Xiang X, Lim KC, Levi G, Clouthier DE (2004) Endothelin-A receptor-dependent and -independent signaling pathways in establishing mandibular identity. *Development* 131(18):4413–4423.
23. Hayashi M, et al. (2007) Comparative roles of Twist-1 and Id1 in transcriptional regulation by BMP signaling. *J Cell Sci* 120(Pt 8):1350–1357.
24. Cai J, Jabs EW (2005) A twisted hand: bHLH protein phosphorylation and dimerization regulate limb development. *BioEssays* 27(11):1102–1106.
25. Bildsoe H, et al. (2009) Requirement for Twist1 in frontonasal and skull vault development in the mouse embryo. *Dev Biol* 331(2):176–188.
26. Connerney J, et al. (2006) Twist1 dimer selection regulates cranial suture patterning and fusion. *Dev Dyn* 235(5):1345–1357.
27. Vincentz JW, et al. (2013) Twist1 controls a cell-specification switch governing cell fate decisions within the cardiac neural crest. *PLoS Genet* 9(3):e1003405.
28. Depew MJ, Simpson CA (2006) 21st century neontology and the comparative development of the vertebrate skull. *Dev Dyn* 235(5):1256–1291.
29. Birnbaum RY, et al. (2012) Functional characterization of tissue-specific enhancers in the DLX5/6 locus. *Hum Mol Genet* 21(22):4930–4938.
30. Kim KS, et al. (2013) Endothelin regulates neural crest deployment and fate to form great vessels through Dlx5/Dlx6-independent mechanisms. *Mech Dev* 130(11-12):553–566.
31. Wolberger C (1996) Homeodomain interactions. *Curr Opin Struct Biol* 6(1):62–68.
32. Feledy JA, Morasso MI, Jang SI, Sargent TD (1999) Transcriptional activation by the homeodomain protein distal-less 3. *Nucleic Acids Res* 27(3):764–770.
33. Pandolfi PP, et al. (1995) Targeted disruption of the GATA3 gene causes severe abnormalities in the nervous system and in fetal liver haematopoiesis. *Nat Genet* 11(1):40–44.
34. He F, et al. (2014) Directed Bmp4 expression in neural crest cells generates a genetic model for the rare human bony syngnathia birth defect. *Dev Biol* 391(2):170–181.
35. Jeong J, et al. (2008) Dlx genes pattern mammalian jaw primordium by regulating both lower jaw-specific and upper jaw-specific genetic programs. *Development* 135(17):2905–2916.
36. Lieuw KH, Li Gl, Zhou Y, Grosveld F, Engel JD (1997) Temporal and spatial control of murine GATA-3 transcription by promoter-proximal regulatory elements. *Dev Biol* 188(1):1–16.
37. Griffin KJ, et al. (2000) A conserved role for H15-related T-box transcription factors in zebrafish and Drosophila heart formation. *Dev Biol* 218(2):235–247.
38. Liu W, et al. (2005) Threshold-specific requirements for Bmp4 in mandibular development. *Dev Biol* 283(2):282–293.
39. Vincentz JW, Barnes RM, Firulli BA, Conway SJ, Firulli AB (2008) Cooperative interaction of Nkx2.5 and Mef2c transcription factors during heart development. *Dev Dyn* 237(12):3809–3819.

Vincentz et al.

www.manaraa.com